Study on the influence of optical absorption on polarization characterization of tissues

Yunfei Wang
Yu Huang
Nan Zeng
Yihong Guo
Yonghong He
Hui Ma

SPIE.

Study on the influence of optical absorption on polarization characterization of tissues

Yunfei Wang,[a,b,†] Yu Huang,[a,c,†] Nan Zeng,[a,b,*] Yihong Guo,[a,b] Yonghong He,[a,b] and Hui Ma[a,b,d,*]
[a]Tsinghua University, Graduate School at Shenzhen, Guangdong Research Center of Polarization Imaging and Measurement Engineering Technology, Shenzhen Key Laboratory for Minimal Invasive Medical Technologies, Shenzhen, China
[b]Tsinghua University, Department of Physics, Beijing, China
[c]Tsinghua University, Department of Biomedical Engineering, Beijing, China
[d]Tsinghua-Berkeley Shenzhen Institute, Center for Precision Medicine and Healthcare, Shenzhen, China

Abstract. Absorption effect is a basic optical phenomenon and an important feature in tissue imaging and characterization. Based on our Monte Carlo simulation on the anisotropic tissue model (sphere-cylinder birefringence model), combined with our experiments of tissue phantoms, we demonstrate the influence of absorption effect on Mueller matrix and particularly on depolarization, linear retardance, and diattenuation parameters. The simulation and experimental results show a good consistency on the suppressed depolarization and scatterering induced retardance, and the enhanced diattenuation caused by the absorption, and also indicate the birefringence induced retardance insensitive to the absorption. Study of the phase function of different incident polarized lights and the distribution of scattering number gives a preliminary explanation about the above results. © The Authors. Published by SPIE under a Creative Commons Attribution 3.0 Unported License. Distribution or reproduction of this work in whole or in part requires full attribution of the original publication, including its DOI. [DOI: 10.1117/1.JBO.23.12.121609]

1 Introduction

Light scattering and absorbing are two main processes of the interaction between light and biological tissues. Generally, the scattering in most of biological tissues can degrade the penetration depth and the image contrast using optical methods. Compared with other techniques, polarization imaging can suppress contributions from multiple scattered photons, and improve the imaging quality for superficial tissues. Moreover, multidimensional description-based Stokes vectors or Mueller matrices can expand the potential of tissue characterization.

Since Bickel confirmed the effectiveness to extract useful information from biological materials by combining polarization and light scattering,[1] many polarization parameters (differential polarization,[2] the degree of polarization,[3,4] Mueller matrix,[5–8] etc.) and polarization scattering models (sphere-birefringence model[9] and sphere-cylinder-scattering model[10–12]) have been put forward to describe the distinctive pathological features. However, for certain biological tissues containing pigment like melanin or chromatophores like chloroplast, the inherent absorbing effect in ambient media or on scatterers make the polarized light propagation in such absorptive media different.

For the absorption effect in ambient media, Li et al. proposed a skin model containing a top isotropic layer, a bottom anisotropic layer, and an absorbing medium to explain the contrast mechanism of polarization imaging for melanoma.[13] Dmitry et al. proposed an approximate expression to describe the dependence of the degree of residual linear polarization on the absorption of scattering media.[14] Swami et al. studied how the absorption of the scattering medium containing spherical scatterers and absorbing medium affects the depolarization.[15] For absorption on the scatterers, Kienle et al. considered the imaginary part of the scatterers' complex refractive index for multiple scattering of polarized light propagation in turbid media, and evaluated the whole angle-dependent Mueller matrix by comparing results of polarization sensitive radiative transfer solution with Maxwell theory.[16] Mishchenko et al. employed the numerically exact superposition T-matrix method to demonstrate that the increasing absorption of particles diminishes and nearly extinguishes certain optical effects such as depolarization and coherent backscattering.[13]

Our previous work has developed an optical scattering model called the sphere-cylinder-birefringence model (SCBM) to simulate and simplify complicate and anisotropic biological tissues.[12] Two sets of polarization parameters extracted from the Mueller matrix transformation and Mueller matrix polar decomposition (MMPD) techniques have been used to test this model and explain some pathological changes.[16–21] However, considering the possible absorption in real biological tissues, it is necessary to include the absorbing effect in this model and explore the consequent change of these polarization parameters. This paper studies the absorption in ambient media and the induced impact on polarization parameters; absorption on the scatterers will be discussed in our further research. A Monte Carlo program was used to trace the polarization status of polarized photons scattered by the spheres and cylinders and propagating in a medium including absorption and birefringent effects. Experiments were carried out on forward scattering Mueller matrix measurements of samples containing polystyrene microspheres, well-aligned glass fibers, and absorbing ink solution. Both experiments and simulation results indicate how the absorption effect during the light transmission affects the MMPD parameters.

---

*Address all correspondence to: Nan Zeng, E-mail: zengnan@sz.tsinghua.edu.cn; Hui Ma, E-mail: mahui@tsinghua.edu.cn

†These authors contributed equally to this work.

2 Theory

2.1 Monte Carlo Simulation and SCBM

MMPD proposed by Lu-Chipman can quantitatively decompose the measured Mueller matrix into the product of three factors to determine its diattenuation, retardance, and depolarization[21]

$$M = M_\Delta M_R M_D. \tag{1}$$

The matrices M_Δ, M_R, and M_D represent the polarization parameters of depolarization, retardance, and diattenuation, respectively. The value of diattenuation D could be calculated from M_D matrix as follows:

$$D = \frac{1}{m_{11}} \sqrt{(m_{12}^2 + m_{13}^2 + m_{14}^2)}. \tag{2}$$

The depolarization coefficient Δ could be determined from the elements of matrix M_Δ:

$$\Delta = 1 - \frac{|tr(M_\Delta) - 1|}{3}. \tag{3}$$

The last MMPD parameter retardance R could be calculated from M_R and is divided into two types of retardance, the linear retardance δ and the circular retardance ψ, which in other words is called optical activity:

$$R = \cos^{-1}\left[\frac{tr(M_R)}{2} - 1\right], \tag{4}$$

$$\delta = \cos^{-1}$$
$$\times \left\{ \sqrt{[M_R(2,2) + M_R(3,3)]^2 + [M(3,2) - M_R(2,3)]^2} - 1 \right\}, \tag{5}$$

$$\psi = \tan^{-1}\left[\frac{M_R(3,2) - M_R(2,3)}{M_R(2,2) + M_R(3,3)}\right]. \tag{6}$$

2.2 Monte Carlo Simulation and SCBM

A Monte Carlo simulation program was used to track and record the polarization status of photons propagating in anisotropic scattering media with optical absorption. This simulation program is on the basis of our previously proposed sphere-cylinder birefringence model (SCBM), which describes the anisotropic media like biological tissues as a mixture consisting of spherical and cylindrical scatterers, corresponding to the microstructural and optical properties of cells and fibrous tissues in organism.[12]

Here, we introduce the absorption effect in the intercellular substance and make it adjustable in this model. Other parameters in this model can also be adjustable to simulate different types of tissue samples. For scatterers, the variable parameters include the sizes, refractive indices, scattering coefficients of spheres and cylinders, and the orientation angular distribution of cylinders. For the surrounding medium, the variable parameters include thickness, refractive index, absorbing coefficient or birefringence, dichroism, and optical activity coefficient.

We calculate the scattering coefficients of spheres based on the known concentration, sphere size, and refractive index according to Mie theory. For the case of a cylinder, the scattering coefficient is not only related to the density, diameter, and refractive index but also varies with incident polarization status and the angle between the direction of incident photon and the cylinder. During calculations, we should first determine this angle according to the spatial orientation of the cylinder and the propagation direction of the photon, and then follow the theory of polarized photon scattering at an infinitely long cylinder, which has been demonstrated in detail in Ref. 13. The scattering coefficient of a microsphere is a constant once its size and refractive index are set. However, the scattering coefficient of cylinders $\mu_{s,\text{cyl}}$ varies with the angle ζ between the direction of incident photon and the cylinder:[11,22]

$$\mu_{s,\text{cyl}}(\zeta) = Q_{\text{sca}}(\zeta) \cdot d \cdot C_A, \tag{7}$$

where d and C_A are the diameter and density of the cylinders. Q_{sca} is the scattering efficiency of a single cylinder. It is a function of the angle ζ and the polarization state of the incident photon. In the program, we first determine ζ according to the spatial orientation of the cylinder and the propagation direction of the photon. The efficiency Q_{sca} can be calculated using the analytic solution of the Maxwell equation.[11,23]

2.3 Experiment Setup

The experiment setup for forward scattering Mueller matrix measurement is shown in Fig. 2. A 3-W LED is used as the light source with its center wavelength of 650 nm. After beam expansion and collimation, the incident light passes through a set of a linear polarizer and quarter wave plate and could be modulated into six types of polarization states: horizontal linear (H), vertical linear (V), 45-deg linear (P), 135-deg linear (M), and right/left circular (R/L). The scattering light exiting from samples is examined by the analyzer, which is also a set of quarter wave plate and linear polarizer, and finally is collected by a lens and recorded by a CCD (Q-imaging Retiga Exi, 12-bit). For each incident polarization state, six components of the forward scattering light are detected through the analyzer. The Mueller matrix can be calculated through the 36 raw images accordingly:

$$M = \begin{pmatrix} m_{11} & m_{12} & m_{13} & m_{14} \\ m_{21} & m_{22} & m_{23} & m_{24} \\ m_{31} & m_{32} & m_{33} & m_{34} \\ m_{41} & m_{42} & m_{43} & m_{44} \end{pmatrix}$$

$$= \frac{1}{2} \begin{pmatrix} HH+HV+VH+VV & HH+HV-VH-VV & PH+PV-MP-MM & RH+RV-LH-LV \\ HH-HV+VH-VV & HH-HV-VH+VV & PH-PV-MH-MV & RH-RV-LH+LV \\ HP-HM+VP-VM & HP-HM-VP+VM & PP-PM-MP+MM & RP-RM-LP+LM \\ VR+HR-LL-RL & VL+HR-HL-VR & ML+PR-PL-MR & RR+LL-LR-RL \end{pmatrix}. \tag{8}$$
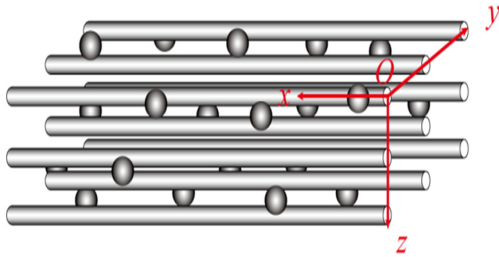
Fig. 1 Schematic of SCBM.

In Eq. (8), the first letter of Mueller elements represents input polarization state, and the second letter represents the states of polarization analyzer. In experiments, we define a reference coordinate system with its x axis parallel to the optical platform and y axis perpendicular to it. As shown in Figs. 1 and 2, the surface of sample is set to $x - y$ plane, and the incident light passes through the sample along z axis.

The measured anisotropic and absorbing samples contain polystyrene microspheres and well-aligned glass fibers immersed in absorbing ink solution. The diameter and refractive index of polystyrene microspheres are 1 μm and 1.59, respectively. The glass fibers, with the diameter of 10 μm and the refractive index of 1.547, are arranged in alignment and wrapped neatly around the metal frame, which is immersed in the middle of the ink solution. The ink solution is configurable for concentration and is filled in a 5 cm × 0.5 cm × 3 cm cuvette. Different concentrations of ink solution represent different absorbing coefficients. The MMPD method is used to characterize the polarization properties of samples and investigate the influence of the absorption effect on corresponding parameters.

3 Results and Discussion

To study the change of full polarization information with the increasing absorption effect, all Mueller matrix elements are simulated using our Monte Carlo polarization scattering simulation program and SBM anisotropic tissue model. Figure 3 shows the spatial distribution spectrum patterns of all Mueller elements. Here, different color curves represent different absorption coefficients. The vertical axes of the subplots represent the analyzed polarized intensity, whose unit is equal to the calculated photon number during the polarized light scattering process. The lateral axis is the spatial location of photon emission, whose value represents the pixel sequence number of the simulated detection plane where the incident spot center is on pixel 100.

Figures 3(a) and 3(b) show two SCBM models with a sphere-cylinder ratio of 10:50 and 30:30, respectively, and Fig. 3(c) shows normalized processed patterns using the same model as Fig. 3(a). We focus on the optical absorption induced polarization characterization for an anisotropic medium. The proportion of cylindrical scatterers is a typical factor to describe the tissue anisotropy according to our previous work,[4] so we study the influence of the anisotropy of scattering media using the two cases of different sphere-cylinder ratios [Figs. 3(a) and 3(b)]. Furthermore, in Fig. 3(c), by normalization, we remove the scattered intensity change due to absorption and make the polarization-related phenomena clear.

From this figure, we can see that most of the elements can be influenced by the interstitial absorption except for m_{13}, m_{14}, m_{31}, and m_{41}, and the tissue model with a high anisotropy will be affected more by comparison of Figs. 3(a) and 3(b). After normalization, we can see that the relative change of nondiagonal elements with the increasing absorption is not so obvious, and the value of diagonal elements on all the spatial locations can be uniformly decreased gradually by absorption. Generally, the additional absorption phenomena in tissue models can cause the scattering intensity change of light with different incident polarization states, implying diattenuation behavior during the light scattering. Also, the apparent change of diagonal elements and the m_{34} and m_{43} indicate the influence of absorption on depolarization and phase retardance processes.

In our previous study, we pointed out that, for SCBM, spherical scatterers only contribute to depolarization, but cylindrical scatterers contribute to diattenuation, depolarization, and partial retardance (the rest comes from birefringence of the medium).[21] Now we consider the influence of the absorbing coefficient of the surrounding medium by MMPD parameters. Figures 4(a)–4(c)
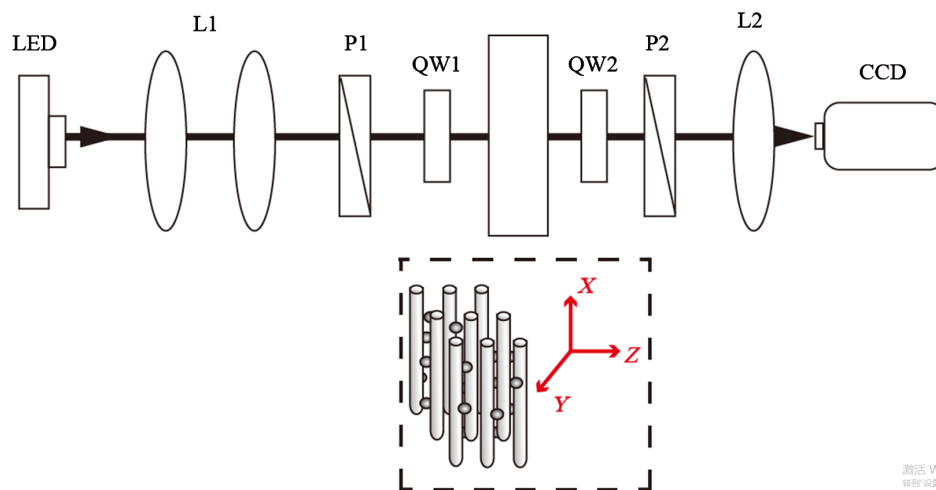
Fig. 2 The forward scattering Mueller matrix measurement setup schematic. LED, light source; L1, L2: lenses; P1, P2: lenses; QW1, QW2: quarter wave plate, the sample position corresponding to Fig. 1 is shown in the dashed frame.
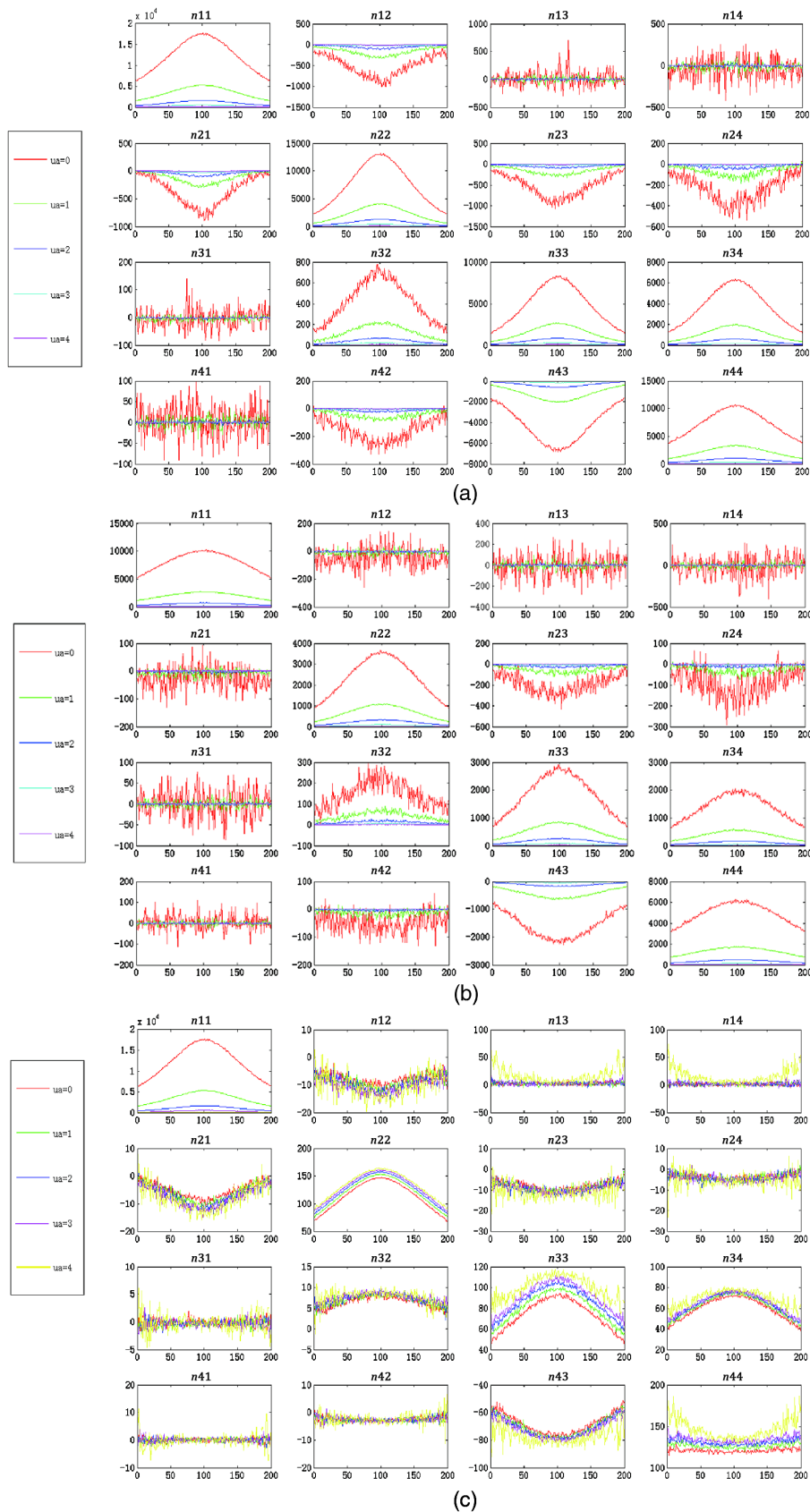
Fig. 3 Spatial distribution patterns of Mueller elements under different optical absorptions based on Monte Carlo simulations of SCBM: (a) SCBM with a sphere-cylinder ratio of 10:50; (b) SCBM with a sphere-cylinder ratio of 30:30; and (c) normalized patterns of (a).
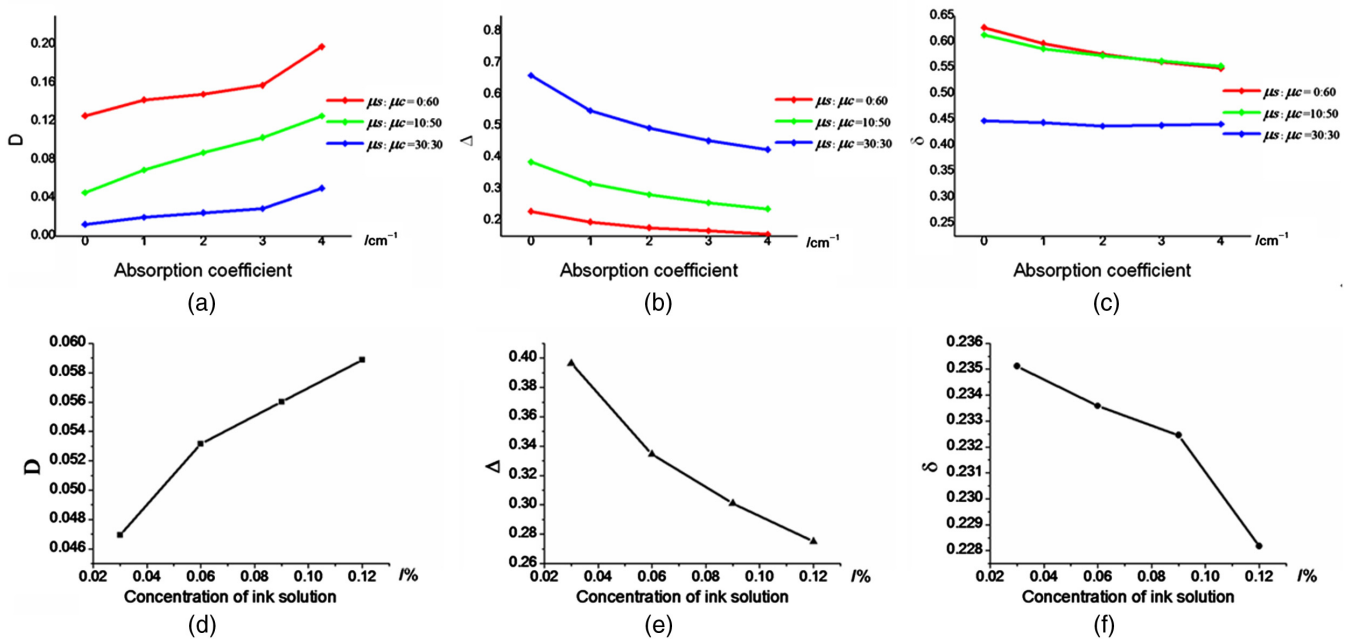
Fig. 4 MMPD results: (a)–(c) Monte Carlo simulation of SCBM and (d)–(f) experiments of sphere-cylinder scattering model.

show simulation results, respectively, of the diattenuation, depolarization, and linear retardance with the increasing absorption. In this SCBM, the diameters of spheres and cylinders are 1 and 10 μm, their refractive indices are 1.59 and 1.547. The birefringence of the ambient medium remains 2×10^{-6}. Considering various tissue anisotropy, we simulated three models marked by different colors in Fig. 4 with different ratios of spherical scattering coefficient and cylindrical scattering coefficient: 0:60, 10:50, and 30:30, respectively. Figures 4(b) and 4(c) clearly point out the negative correlation between the depolarization and the linear retardance parameters with the absorption coefficient. On the contrary, the diattenuation values due to cylinders show a positive correlation with absorption. Moreover, the enhanced diattenuation and the weakened retardance seem more obvious for the scattering model with a higher anisotropy. We use polystyrene microspheres and glass fibers to mimic spherical and cylindrical scatterers for the experimental verification, shown in Figs. 4(d)–4(f). When preparing the polyacrylamide gel, for the stability of the gelation process, we can employ only diluted ink solution to introduce the absorption effect of the surrounding media. As for glass fibers, we wrap them in alignment around a metal frame and then immerse them in the middle of the microsphere solution containing the ink solution. Compared with simulations, the linear retardance is smaller because we cannot simultaneously introduce absorption and birefringence into the surrounding medium in experiments. However, the results still reveal the similar regularity that the increasing absorption enhances the diattenuation but depresses retardance and depolarization.

For SCBM, we also can modify the tissue anisotropy by the spatial orientation distribution of cylinders. We assume that the orientation of cylindrical scatterers follows a Gaussian distribution function and the FWHM of this function can be used to describe the order of alignment. A bigger FWHM means a more disordered distribution of cylinders, which can significantly reduce the anisotropy of system. So we can simulate the influence on MMPD characters of the absorption coefficient

with different orientation distributions of cylinders, as shown in Figs. 5(a)–5(c), where the FWHM of the cylinder distribution function is set to 5 deg, 10 deg, and 20 deg, and their main orientations are along with the direction of x axis shown in Fig. 1. The scattering coefficients of spheres and cylinders are, respectively, 10 and 50 cm^{-1}. Their diameters are, respectively, 1 and 10 μm. The birefringence of ambient medium is set to 2×10^{-6}. Similarly with Fig. 4, for one thing, these results confirm again that the absorption effect in the ambient medium can surely enhance the diattenuation but reduce depolarization and linear retardance. For another, the influence of the optical absorption effect also varies with different degrees of tissue anisotropy. In Figs. 5(a) and 5(c), the change of diattenuation and linear retardance is clearer for the red line with the smallest FWHM value meaning a more orderly arrangement of cylinders. In order to exclude the distinctiveness of the above simulation results on absorption caused by the main orientation angle of cylinders, we set other three different orientation angles in the following simulations. As shown in Figs. 5(d)–5(f), the red, green, and blue lines, respectively, represent the simulation with the main orientation angle of 0 deg, 30 deg, and 45 deg between the axial direction of cylinders and x axis. It can be seen that the qualitative impact of absorption effects on decomposition parameters remains the same.

Next, we consider another anisotropic factor in our SCBM tissue model, i.e., the birefringence effect in the ambient medium. As shown in Fig. 6, we change the absorption coefficient in our SCBM models with different birefringence of 0, 2×10^{-6}, 4×10^{-6} colored with red, green, blue markers in sequence. The diameters of spheres and cylinders are, respectively, 1 and 10 μm, and the scattering coefficient of spheres and cylinders are, respectively, 10 and 50 cm^{-1}. The FWHM of cylinder orientation distribution function remains 5 deg. Here the red line with $\Delta n = 0$ shows the linear retardance totally produced by cylinder scattering; the retardance difference among different color results originates from the birefringence induced retardance. Consistent with the above figures, the
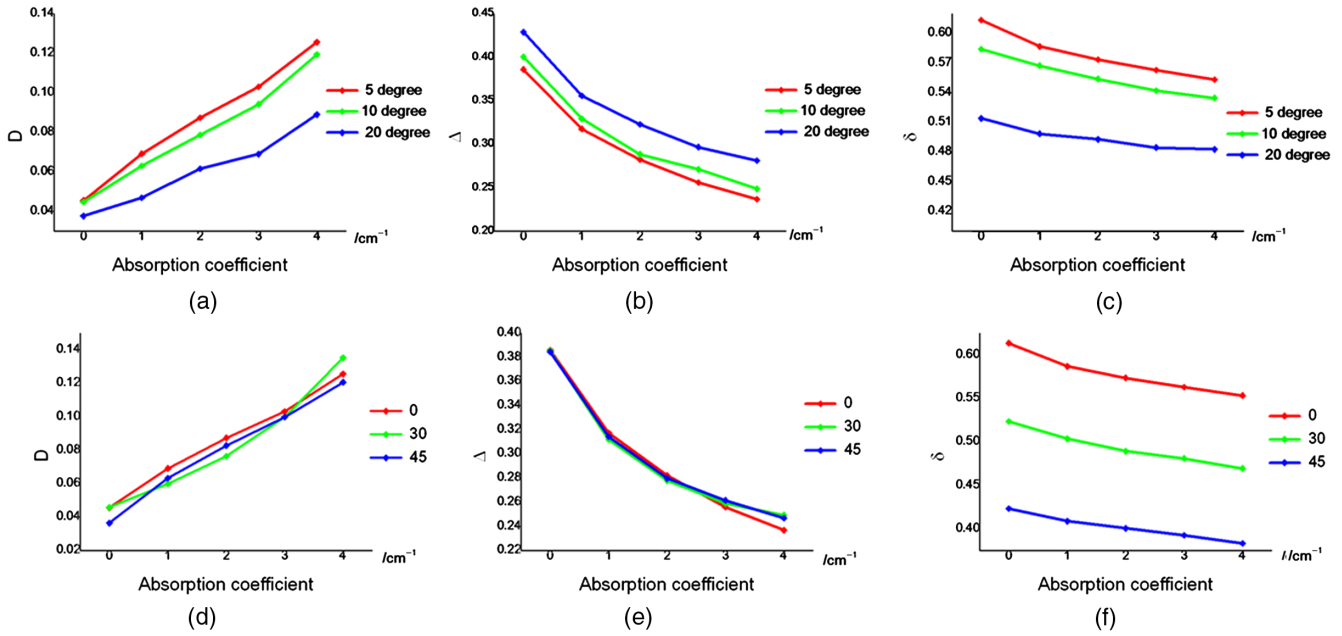
Fig. 5 MMPD results: (a)–(c) Monte Carlo simulation of SCBM with different FWHM of cylinder orientation distribution function while the main orientation remains the direction of *x* axis. (d)–(f) Monte Carlo simulation of SCBM with different main orientation angles of cylinders while the FWHM of the orientation distribution function remains 5 deg.
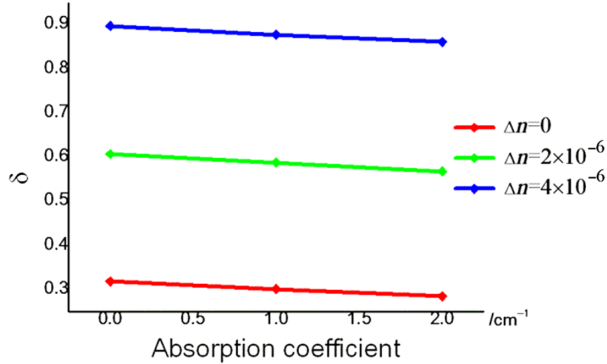
Fig. 6 MMPD results of SCBM with different birefringence in ambient medium.

optical absorption can cause decreased retardance, however, the parallel colored lines in Fig. 6 imply that the influence of absorption on retardance parameter is independent with the birefringence effect in the surrounding medium, and the decrease of the shown retardance curves is due to the depressed scattering process by absorption.

Combined with the above three figures, we can find that the additional optical absorption do have impact on polarization processes and apparently depress the depolarization and linear retardance, however, enhance the biattenuation. By comparison, the influence of absorption varies with the degree of scattering anisotropy in the simulated tissue models and SCBM models with more cylindrical elements or a highly ordered orientation seem sensitive to the optical absorption. The existence of birefringence and the main orientation angle do not affect how MMPD parameters change with the absorption coefficient, and conversely the optical absorption cannot change the contribution of birefringence on tissue anisotropy.

The following discussions try to explain the impact of absorption effect in ambient medium on scattering induced diattenuation, depolarization, and linear retardance. First, for diattenuation, we start from its definition as

$$D = \frac{\sqrt{(m_{12}^2 + m_{13}^2 + m_{14}^2)}}{m_{11}}. \quad (9)$$

In SCBM, when the orientation of the cylinder is set along *x* axis, we can approximate D as the following expression considering the value of matrix element m_{13} and m_{14} are much smaller than that of m_{12}:

$$D = \frac{|m_{12}|}{m_{11}} = \frac{|\mathrm{HI} - \mathrm{VI}|}{\mathrm{HI} + \mathrm{VI}}. \quad (10)$$

Here "HI" represents the intensity of scattered light in the case of the horizontal polarized incident light, and "VI" represents the intensity of scattered light in the case of the vertical polarized incident light. Using one set of the above data as an example, in which the scattering coefficients of spheres and cylinders are 10 and 50 cm^{-1}, the FWHM of cylinders orientation distribution function is 5 deg, and the birefringence of ambient medium is 2×10^{-6}, we investigate how the $|\mathrm{HI} - \mathrm{VI}|/(\mathrm{HI} + \mathrm{VI})$ vary with the absorption coefficient. As shown in Fig. 7(a), $|\mathrm{HI} - \mathrm{VI}|/(\mathrm{HI} + \mathrm{VI})$ show the same changing trend as the red line in Fig. 5(a), which confirms that D reflects the scattering difference for two orthogonal linear polarization incidences in this model, like Fig. 7(b). Theoretically for isotropic scattering media without irregular scatterers and optical anisotropy, the scattered photon behaviors of orthogonal linear polarization incidence light are equal. However, the existence of anisotropic factors in the tissue model, like cylindrical scatterers, can cause polarization response during scattering sensitive to the incident polarization

(a)

(b)

(c)
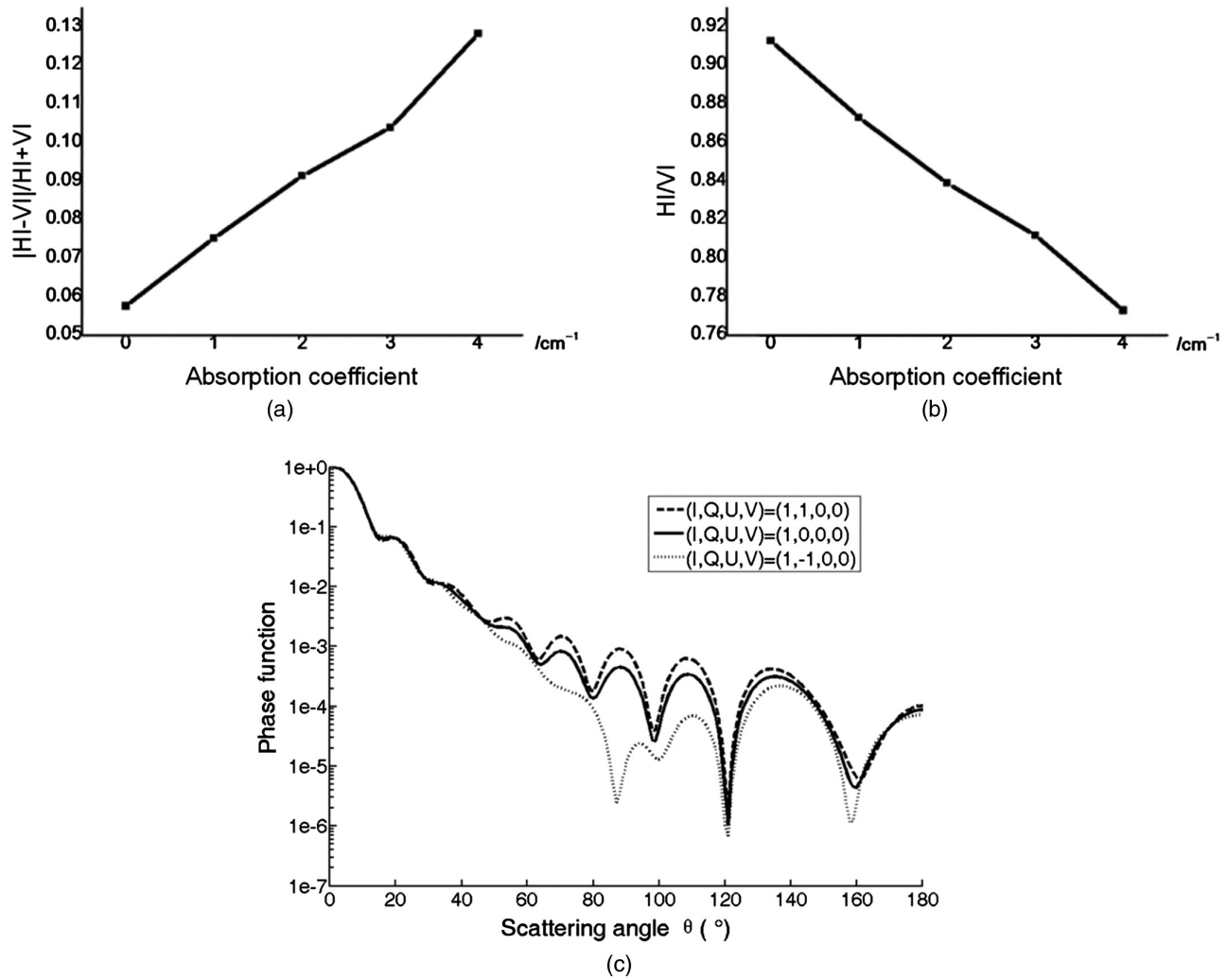
Fig. 7 (a) and (b) The function of $|HI - VI|/(HI + VI)$ and HI/VI with absorption coefficient and (c) the scattering phase function of cylinder.

status. As shown in Fig. 7(c), we can see that the phase function of cylinder depends on the polarization state of incident light. When the scattering angle ranges from 0 deg to 45 deg, the horizontal polarized light has nearly the same phase function as the vertical polarized light. While when the scattering angle ranges from 45 deg to 90 deg, the phase function of the horizontal polarized light is clearly bigger than that of the vertical polarized light, thus indicating a bigger lateral scattering possibility for horizontal polarized incident light. Correspondingly during the scattering process, the horizontal polarized incident light may undergo more lateral scattering steps and has a longer optical path when scattered by cylindrical scatterers. As a consequence, the scattered behavior of horizontal polarized light will be more affected than the vertical polarized light by the absorption effect in the ambient medium, which leads to the enhanced difference of HI and VI and finally produces a bigger diattenuation.

In order to explain the impact of absorption on scattering induced depolarization and linear retardance, we analyze the photon behaviors in SCBM with various absorption extents shown in Fig. 8. As we can see, the enhanced absorption depresses the multiscattered photons more and thus results in decreased total scattering numbers. For the absorption effect
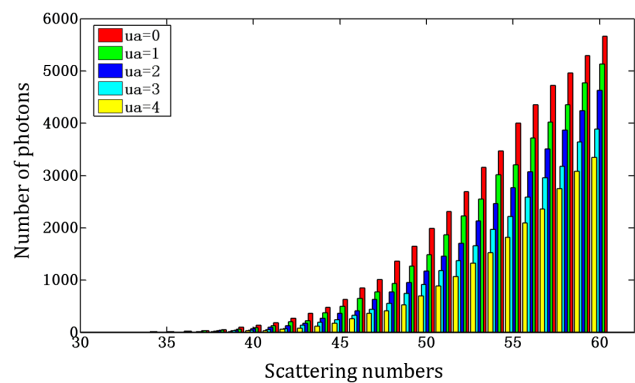
Fig. 8 The distribution of the scattering number of the forward scattering photons.

in the surrounding media, the absorption can cause additional light attenuation between one and the next scattering event. So the multiple scattered photons mean more absorption probability and show a clearly declined proportion with the increase of the absorption setting value. For the SCBM tissue model and the forward detection scheme, not only is the depolarization
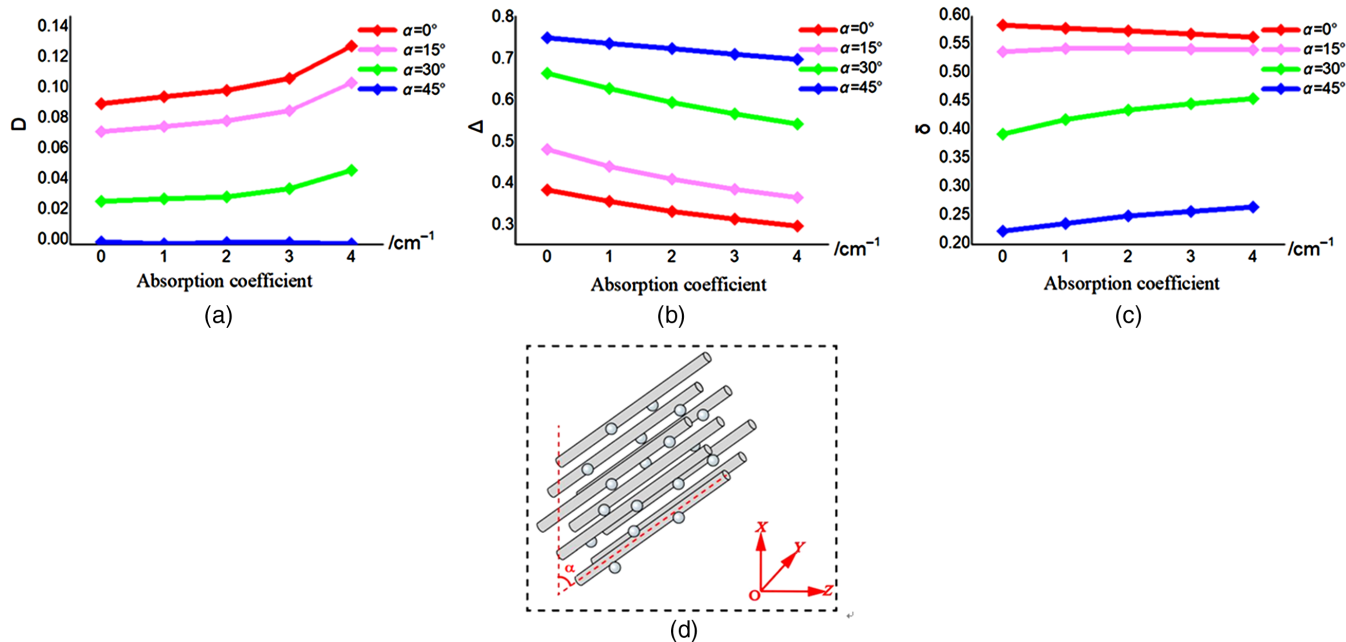
Fig. 9 MMPD results: (a)–(c) Monte Carlo simulation of SCBM with different orientation angles on $x - z$ plane and (d) schematic diagram of SCBM model.

phenomena related to the multiple scattering, but also the phase retardance is contributed by the scattering of anisotropic cylinders, so the depressed multiple scattering by absorption can produce a lower depolarization and retardance.

Finally, we pay attention to the cylindrical scatterers with the special orientation angles not on the surface plane, as shown in Fig. 9. It can be seen that the change trend of diattenuation and depolarization items [Figs. 9(a) and 9(b)] seems similar to Fig. 5. So, the discussion about the influence of optical absorption on these two processes is still valid even for the fibrous microstructures not perpendicular to the incident light and not on the surface plane. However, as shown in Fig. 9(c), the phase retardance increases along with the increasing absorption. These simulation results seem different from the case of cylinders perpendicular to incident light, but actually, we can provide an explanation based on our previous research.[24] Concretely, the total retardance depends on the coupling of two parts of retardances, respectively, from birefringence and cylindrical scatterers, closely related to the interception angle between the orientation of birefringence and cylinders. Based on the above results and discussions in this paper, the cylinder induced retardance can be decreased due to the reduced scattering times by absorption. But for the case of Figs. 9(a)–9(c), the main orientation angle of cylinders is on $x - z$ plane and the interception angle from the birefringence axis (x axis) is equal to 90 deg, where the retardance induced by birefringence and cylinders will cancel each other first, as demonstrated in Ref. 24. It means that even less contribution from cylinders could restrain such canceling out between different retardance sources and cause the enhanced total retardance, which can explain the increased simulated retardance in Fig. 9(c) in this paper with the increasing optical absorption.

4 Conclusion

In this paper, we focus on the influence of absorption effect on Mueller matrix. By Monte Carlo simulation on our previously proposed SCBM and forward scattering experiments on phantoms containing polystyrene microspheres, well-aligned glass fibers, and ink solution, we analyze the changing trend of Mueller matrix and MMPD parameters with the absorption coefficient. Both simulation and experiment results can indicate that optical absorption in the medium can cause an enhanced diattenuation evaluation and reduce the scattering induced depolarization and linear retardance. The increasing diattenuation can be explained by the different scattering phase functions of cylindrical scatterers for horizontal polarized incident light and vertical polarized incident light. The weakened depolarization and linear retardance should be due to the decrease of multiple scattering photons. However, the linear retardance caused by the intrinsic birefringence in the medium is insensitive to the absorption effect. These simulations and experiments imply that optical absorption affects the change regularity of polarization state of polarized light in tissues, and also show possible potential of polarization parameters used in tissue characterization involving absorption effect.

Disclosures

The authors have no relevant financial interests in this article and no potential conflicts of interest to disclose.

References

1. W. S. Bickel et al, "Application of polarization effects in light scattering: a new biophysical tool," *Proc. Natl. Acad. Sci. U.S.A.* **73**(2), 486–490 (1976).
2. R. R. Anderson, "Polarized light examination and photography of the skin," *Arch. Dermatol.* **127**(7), 1000–1005 (1991).

3. S. L. Jacques, J. R. Roman, and K. Lee, "Imaging superficial tissues with polarized light," *Lasers Surg. Med.* **26**(2), 119–129 (2000).

4. S. L. Jacques, J. C. Ramella-Roman, and K. Lee, "Imaging skin pathology with polarized light," *J. Biomed. Opt.* **7**(3), 329–340 (2002).

5. N. Ghosh and I. A. Vitkin, "Tissue polarimetry: concepts, challenges, applications, and outlook," *J. Biomed. Opt.* **16**(11), 110801 (2011).

6. B. D. Cameron, Y. Li, and A. Nezhuvingal, "Determination of optical scattering properties in turbid media using Mueller matrix imaging," *J. Biomed. Opt.* **11**(5), 054031 (2006).

7. T. Novikova et al, "The origins of polarimetric image contrast between healthy and cancerous human colon tissue," *Appl. Phys. Lett.* **102**(24), 241103 (2013).

8. Y. A. Ushenko et al, "Muellermatrix diagnostics of optical properties of polycrystalline networks of human blood plasma," *Opt. Spectrosc.* **112**(6), 884–892 (2012).

9. L. H. Wang, S. L. Jacques, and L. Zheng, "Monte Carlo modeling of photon transport in multilayered tissues," *Comput. Methods Programs Biomed.* **47**, 131–146 (1995).

10. H. He et al., "Two-dimensional backscattering Mueller matrix of sphere-cylinder scattering medium," *Opt. Lett.* **35**(14), 2323–2325 (2010).

11. T. Yun et al., "Monte Carlo simulation of polarized photon scattering in anisotropic media," *Opt. Express* **17**(19), 16590–16602 (2009).

12. E. Du et al, "Two-dimensional backscattering Mueller matrix of sphere-cylinder birefringence media," *J. Biomed. Opt.* **17**(12), 126016 (2012).

13. D. Li et al., "Influence of absorption in linear polarization imaging of melanoma tissues," *J. Innovative Opt. Health Sci.* **7**, 1450009 (2014).

14. D. N. Agafonov et al., "Influence of absorption on residual polarization of backscattered linearly polarized light," *Int. Soc. Opt. Photonics* 166–172 (2002).

15. M. K. Swami et al., "Mueller matrix measurements on absorbing turbid medium," *Appl. Opt.* **49**(18), 3458–3464 (2010).

16. A. Hohmann et al., "Multiple scattering of polarized light: influence of absorption," *Physics in medicine and biology* **59**(11), 2583–2597 (2014).

17. M. I. Mishchenko, L. Liu, and J. W. Hovenier, "Effects of absorption on multiple scattering by random particulate media: exact results," *Optics express* **15**(20), 13182–13187 (2007).

18. E. Du et al., "Mueller matrix polarimetry for differentiating characteristic features of cancerous tissues," *J. Biomed. Opt.* **19**(7), 076013 (2014).

19. Y. Guo et al, "A study on forward scattering Mueller matrix decomposition in anisotropic medium," *Opt. Express* **21**(15), 18361–18370 (2013).

20. S. Y. Lu and R. A. Chipman, "Interpretation of Mueller matrices based on polar decomposition," *J. Opt. Soc. Am. A* **13**(5), 1106–1113 (1996).

21. H. He et al., "A possible quantitative Mueller matrix transformation technique for anisotropic scattering media," *Photonics Lasers Med.* **2**(2), 129–137 (2013).

22. A. Kienle et al, "Light propagation in dentin: influence of microstructure on anisotropy," *Phys. Med. Biol.* **48**, N7–N14 (2003).

23. C. F. Bohren and D. R. Huffman, "*Absorption and Scattering of Light by Small Particles*," John Wiley and Sons, New York (1983).

24. Y. H. Guo et al., "Retardance of bilayer anisotropic samples consisting of well-aligned cylindrical scatterers and birefringent media," *J. Biomed. Opt.* **21**(5), 055002 (2016).

Nan Zeng received her PhD from Tsinghua University, Beijing, China, in 2005. Currently, she is an associate professor in the Graduate School at Shenzhen, Tsinghua University, Shenzhen, China. Her research interests include noninvasive online aerosol analysis and tissue characterization using polarization equipment and simulations.

Hui Ma received his PhD in atomic and molecular physics from Imperial College London, UK, in 1988. He joined the Department of Physics, Tsinghua University, China, in 1991 and moved to Shenzhen in 2003. Currently, he is a professor with the Tsinghua Graduate School at Shenzhen, China, and the Tsinghua-Berkeley Shenzhen Institute, Shenzhen, China. His research interests include polarimetry techniques and their applications which include diagnosis and staging of cancers, differentiation of marine particles and algae, and tracing micron-scale pollutant particles in air.

Biographies for the other authors are not available.